Heavy quark and quarkonium production in the Regge limit of QCD

V. A. Saleev

Samara State University, Samara, Russia

in collaboration with

D. V. Vasin (Samara State University, Samara) and B. A. Kniehl (Hamburg University, Hamburg)

1. QMRK approach
2. Heavy quark production by reggeized gluons
3. Fragmentation approach for heavy meson production
4. B- and D-meson production at the Tevatron and at the LHC
5. NRQCD
6. Heavy quarkonium production by reggeized gluons
7. Heavy quarkonium production at the Tevatron and at the LHC

The QMRK approach

$\mu \approx M_T = \sqrt{M^2 + |\mathbf{p}_T|^2}$

In the conventional Parton Model (PM): Dokshitzer-Gribov-Lipatov-Altarelli-Parisi (DGLAP) evolution equation, $\ln(\mu/\Lambda_{QCD})$.

$S > \mu^2 \gg \Lambda^2_{\rm QCD}$, and $q_T = 0$.

In the high-energy Regge limit the summation of the large logarithms $\ln(\sqrt{S}/\mu)$ in the evolution equation can be more important: Balitsky-Fadin-Kuraev-Lipatov (BFKL) evolution equation and $q_T \neq 0$ for *reggeized* t-channel gluons.

$x = \mu/\sqrt{S} \ll 1$

As the theoretical framework of high-energy factorization scheme we consider the quasi-multi-Regge kinematics (QMRK) approach [Lipatov, Kuraev, Fadin].

QMRK is based on effective quantum field theory implemented with the non-abelian gauge-invariant action, as was suggested a few years ago [Lipatov, 1995].

In the QMRK approach, $q^2 = q_T^2 = -|\mathbf{q}_T|^2 \neq 0$.

The unintegrated gluon distribution function $\Phi(x, |\mathbf{q}_T|^2, \mu^2)$ is used.

In the stage of the numerical calculations, we have used the unintegrated gluon distribution functions $\Phi(x, |\mathbf{q}_T|^2, \mu^2)$ JB , JS , and KMR.

V. A. Saleev and D. V. Vasin:

1) Phys. Rev. D **68**, 114013 (2003);
2) Phys. Atom. Nucl. **68**, 94 (2005) [Yad. Fiz. **68**, 95 (2005)];
3) In Proc. of First Int. Workshop "HSQCD 2004", 73 (2004);
4) Phys. Lett. B **605**, 311 (2005);

B. A. Kniehl, V. A. Saleev and D. V. Vasin:

5) Phys. Rev. D **73**, 074022 (2006).
6) Phys. Rev. D **74**, 014024 (2006).

We have shown that only Kimber(Watt)-Martin-Ryskin unDF describes all data for heavy quark and quarkonium production well.

In 2005 the Feynman rules for the effective theory based on the non-abelian gauge-invariant action were derived for the induced and the some important effective vertices [Antonov, Kuraev, Lipatov, Cherednikov].

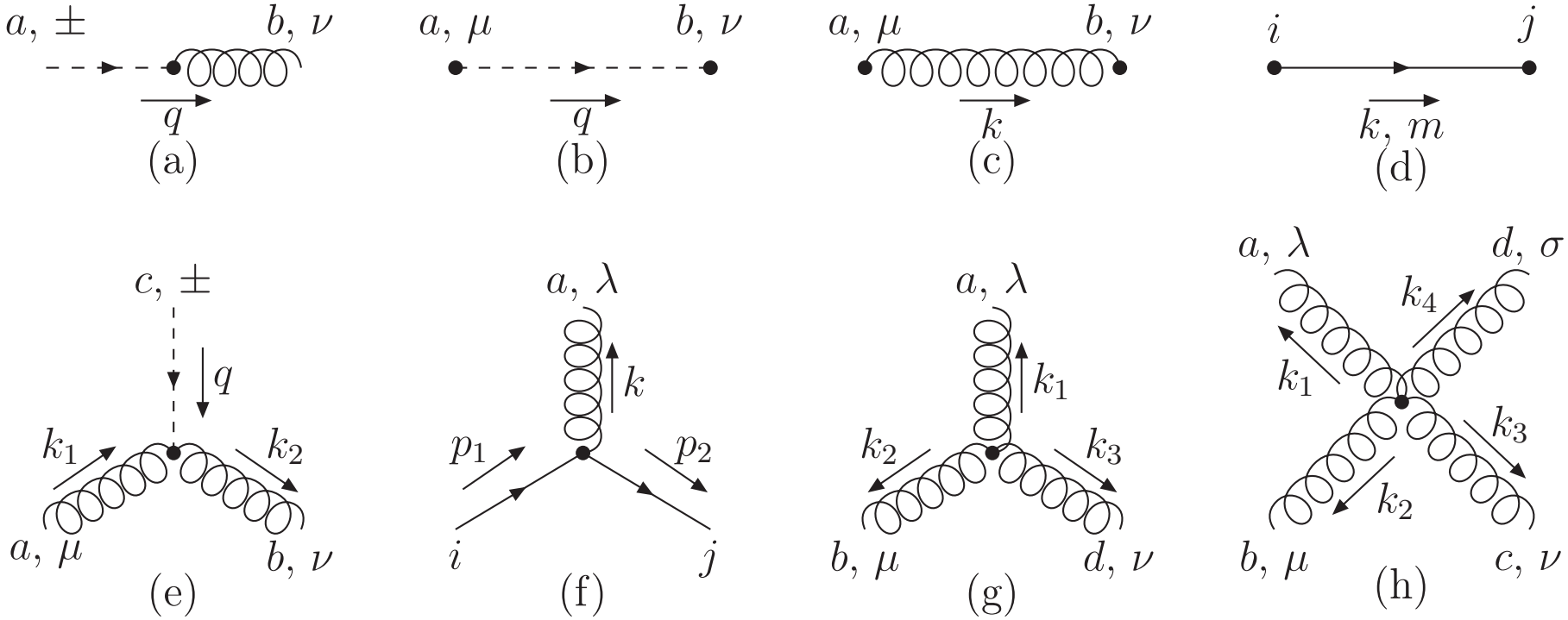

Feynman rules.

The induced vertices of reggeized gluon transition to Yang-Mills gluon $R^{\pm} \to g$ (PR-vertices) has the form:

$$\Gamma^{\pm\nu}_{ab}(q) = i\delta^{ab} q^2 (n^{\pm})^{\nu}, \tag{1}$$

$(n^+)^\nu = P_1^\nu / E_1, \quad P_1 = E_1(1,0,0,1)$

$(n^-)^\nu = P_2^\nu / E_2, \quad P_2 = E_2(1,0,0,-1)$

$(n^+ n^-) = 2, \; (n^\pm n^\pm) = 0,$

k^μ: $k^\pm = (k n^\pm)$.

$q_1 = q_{1T} + \frac{q_1^-}{2} n^+ = q_{1T} + x_1 P_1,$

$q_2 = q_{2T} + \frac{q_2^+}{2} n^- = q_{2T} + x_2 P_2,$

$q_1^+ = q_2^- = 0.$

The induced interaction vertices of reggeized gluon with two Yang-Mills gluons (PPR-vertices) reads:

$$\Gamma^{\mu\pm\nu}_{acb}(k_1,q,k_2) = -g_s f^{abc}\frac{q^2}{k_1^{\pm}}(n^{\pm})^{\mu}(n^{\pm})^{\nu}. \tag{2}$$

The reggeized gluon propagator is specified as follows:

$$D^{\mu\nu}_{ab}(q) = -i\delta^{ab}\frac{1}{2q^2}\left[(n^{+})^{\mu}(n^{-})^{\nu} + (n^{+})^{\nu}(n^{-})^{\mu}\right]. \tag{3}$$

The effective 3-vertices, which describes the production of a single gluon with momentum $k = q_1 + q_2$ and color index b in the "two reggeons collision" $R^+R^- \to g$ (PRR-vertices):

$$\Gamma^{+\mu-}_{cba}(q_1, k, q_2) =$$
$$= V^{\eta\nu\mu}_{cab}(-q_1, -q_2, k)(n^+)^\eta (n^-)^\nu + \Gamma^{\eta-\mu}_{cab}(q_1, q_2, k)(n^+)^\eta + \Gamma^{\nu+\mu}_{acb}(q_2, q_1, k)(n^-)^\nu =$$
$$= 2g_s f^{cba}\left[(n^-)^\mu\left(q_2^+ + \frac{q_2^2}{q_1^-}\right) - (n^+)^\mu\left(q_1^- + \frac{q_1^2}{q_2^+}\right) + (q_1 - q_2)^\mu\right].$$

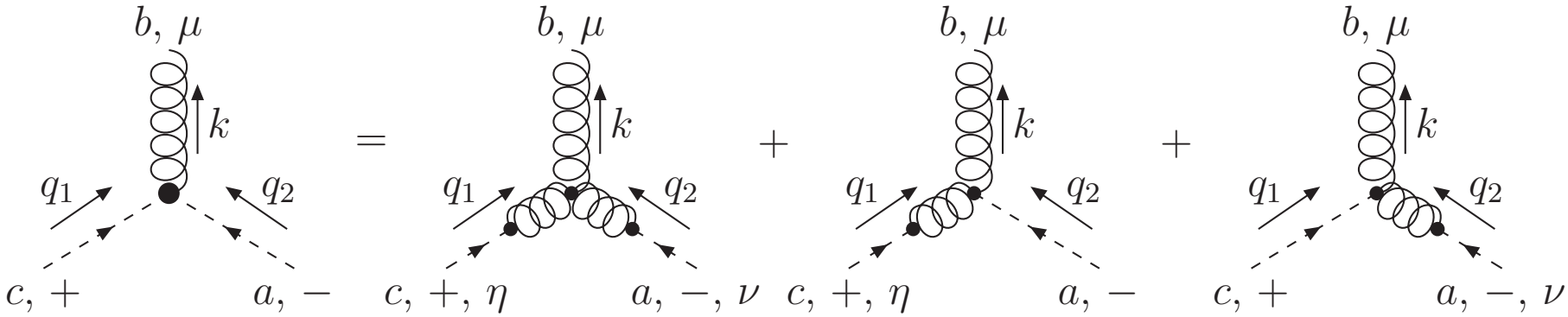

Effective vertex $R^+R^- \to g$.

The gauge invariance of the effective theory leads to the following condition for amplitudes in the QMRK:

$$\lim_{|\mathbf{q}_{1T}|,|\mathbf{q}_{2T}|\to 0} \overline{|\mathcal{A}(R+R\to\mathcal{H}+X)|^2} = 0. \tag{4}$$

In the QMRK approach, the hadronic cross section of quarkonium ($\mathcal{H}$) production in the process

$$p+p\to\mathcal{H}+X \tag{5}$$

and the partonic cross section for the reggeized-gluon fusion subprocess

$$R+R\to\mathcal{H}+X \tag{6}$$

are connected as

$$d\sigma(p+p\to\mathcal{H}+X) = \int\frac{dx_1}{x_1}\int\frac{d^2\mathbf{q}_{1T}}{\pi}\Phi(x_1,|\mathbf{q}_{1T}|^2,\mu^2)\times$$
$$\int\frac{dx_2}{x_2}\int\frac{d^2\mathbf{q}_{2T}}{\pi}\Phi(x_2,|\mathbf{q}_{2T}|^2,\mu^2)\times d\hat{\sigma}(R+R\to\mathcal{H}+X), \tag{7}$$

$x_1=\dfrac{q_1^-}{2E_1}$, $x_2=\dfrac{q_2^+}{2E_2}$.

$$xG(x,\mu^2) = \int \frac{d^2\mathbf{q}_T}{\pi}\Phi(x,|\mathbf{q}_T|^2,\mu^2), \tag{8}$$

The partonic cross section for the two reggeized gluon collision can be presented as follows:

$$d\hat{\sigma}(R+R\to\mathcal{H}+X) = \frac{\mathcal{N}}{2x_1x_2S}\times$$
$$\overline{|\mathcal{A}(R+R\to\mathcal{H}+X)}d\Phi, \tag{9}$$

$$\mathcal{N} = \frac{(x_1x_2S)^2}{16|\mathbf{q}_{1T}|^2|\mathbf{q}_{2T}|^2}. \tag{10}$$

So that when $\mathbf{q}_{1T} = \mathbf{q}_{2T} = 0$ we obtain the conventional factorization formula of the collinear parton model:

$$d\sigma(p+p\to\mathcal{H}+X) =$$
$$\int dx_1 G(x_1,\mu^2)\int dx_2 G(x_2,\mu^2)\times$$
$$d\hat{\sigma}(g+g\to\mathcal{H}+X) \tag{11}$$

The QMRK approach gives the following:

1. The new set of Feynman's rules for the gauge invariant amplitudes with reggeized gluons (and reggeized quarks).

2. The opportunity to perform calculations in the NLO approximation in α_s.

Heavy quark production by reggeized gluons

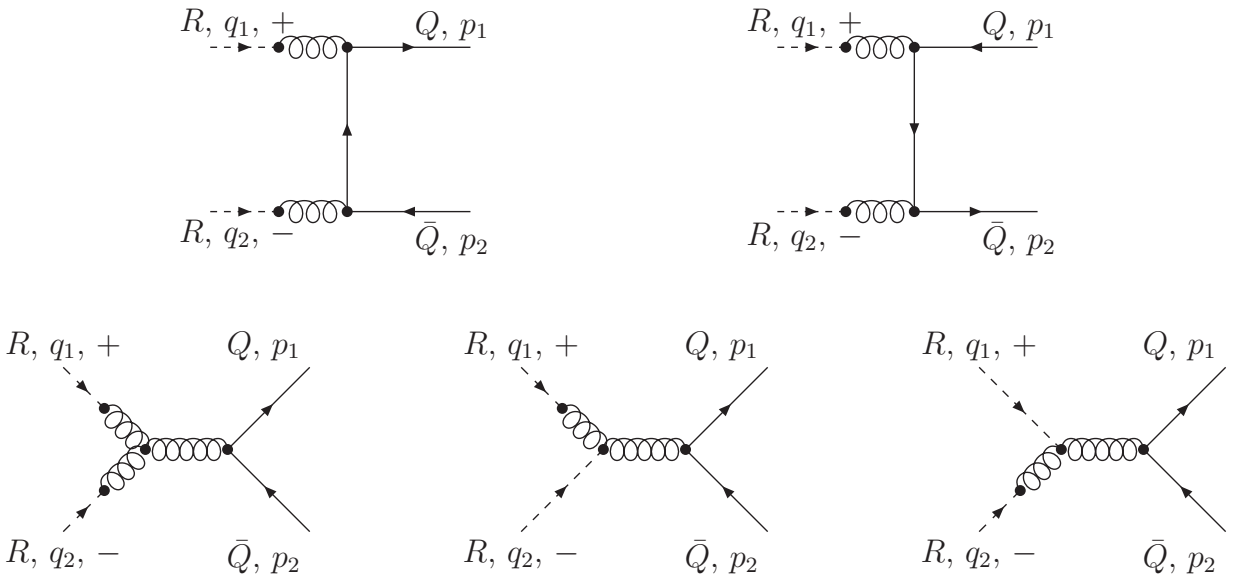

Figure 1: The set of diagrams for $R + R \to Q + \bar{Q}$

$$A_1 = -ig^2 T^a T^b \bar{\mathcal{U}}(p_1,m)\gamma^\alpha \frac{\hat{p}_1 - \hat{q}_1 + m}{(p_1-q_1)^2 - m^2}\gamma^\beta \mathcal{V}(p_2,m)(n^+)^\alpha (n^-)^\beta, \quad (12)$$

$$A_2 = -ig^2 T^b T^a \bar{\mathcal{U}}(p_1,m)\gamma^\beta \frac{\hat{p}_1 - \hat{q}_2 + m}{(p_1-q_2)^2 - m^2}\gamma^\alpha \mathcal{V}(p_2,m)(n^+)^\alpha (n^-)^\beta, \quad (13)$$

$$A_3 = 2g^2 T^c f^{acb} \bar{\mathcal{U}}(p_1,m)\gamma^\delta \mathcal{V}(p_2,m)\frac{1}{(p_1+p_2)^2}$$
$$\times \left[(n^-)^\delta \left(q_2^+ + \frac{q_2^2}{q_1^-}\right) - (n^+)^\delta \left(q_1^- + \frac{q_1^2}{q_2^+}\right) + (q_1-q_2)^\delta\right]. \quad (14)$$

$$\overline{|\mathcal{A}(R+R\to Q+\bar{Q}|^2} = 256\pi^2\alpha_s^2\left(\frac{1}{2N_c}\mathcal{A}_{\rm Ab}+\frac{N_c}{2(N_c^2-1)}\mathcal{A}_{\rm NAb}\right) \tag{15}$$

$$\mathcal{A}_{\rm Ab} = \frac{t_1t_2}{\tilde{t}\tilde{u}} - \left(1+\frac{p_2^+}{\tilde{u}}(q_1^- - p_2^-)+\frac{p_2^-}{\tilde{t}}(q_2^+-p_2^+)\right)^2 \tag{16}$$

$$\begin{aligned}\mathcal{A}_{\rm NAb} &= \frac{2}{S^2}\left(\frac{p_2^+(q_1^- - p_2^-)S}{\tilde{u}}+\frac{S}{2}+\frac{\Delta}{\hat{s}}\right)\left(\frac{p_2^-(q_2^+ - p_2^+)S}{\tilde{t}}+\frac{S}{2}-\frac{\Delta}{\hat{s}}\right)\\ &-\frac{t_1t_2}{q_1^-q_2^+\hat{s}}\left(\left(\frac{1}{\tilde{t}}-\frac{1}{\tilde{u}}\right)(q_1^-p_2^+ - q_2^+p_2^-)+\frac{q_1^-q_2^+\hat{s}}{\tilde{t}\tilde{u}}-2\right)\end{aligned} \tag{17}$$

$$\Delta = \frac{S}{2}\left(\tilde{u}-\tilde{t}+2q_1^-p_2^+-2q_2^+p_2^-+t_1\frac{q_2^+-2p_2^+}{q_2^+}-t_2\frac{q_1^- - 2p_2^-}{q_1^-}\right) \tag{18}$$

Fragmentation approach for heavy meson production

B. A. Kniehl, G. Kramer, I. Schienbein, H. Spiesberger

$$d\sigma(ij \to HX) = \sum_k \int d\sigma(ij \to kX) D_{k\to H}(z,\mu^2) dz \tag{19}$$

$$\mu^2 \frac{dD_k(z,\mu^2)}{d\mu^2} = \sum_i \int_z^1 \frac{dx}{x} P_{ik}(\frac{z}{x}) D_i(x,\mu^2), \tag{20}$$

$$\text{where} \qquad k = q, g, c \tag{21}$$

$$D_c(z,\mu_0^2) = N \frac{z(1-z)^2}{[(1-z)^2+\epsilon z]^2}, \qquad D_{g,q}(z,\mu_0^2) = 0 \tag{22}$$

$$D_b(z,\mu_0^2) = N z^\alpha (1-z)^\beta, \tag{23}$$

B. A. Kniehl and G. Kramer, PR D74, 037502 (2006)

Universal LO nonperturbative $D-$meson fragmentation functions, by fitting e^+e^- data taken by the OPAL Collaboration at CERN LEP1

H_c	Q	N	α	β	ϵ
D^0	c	0.694			0.101
	b	81.7	1.81	4.95	
D^+	c	0.282			0.104
	b	52.0	2.33	5.10	
$D^{\star+}$	c	0.174			0.0554
	b	69.5	2.77	4.34	
D_s^+	c	0.0498			0.0322
	b	27.5	1.94	4.28	

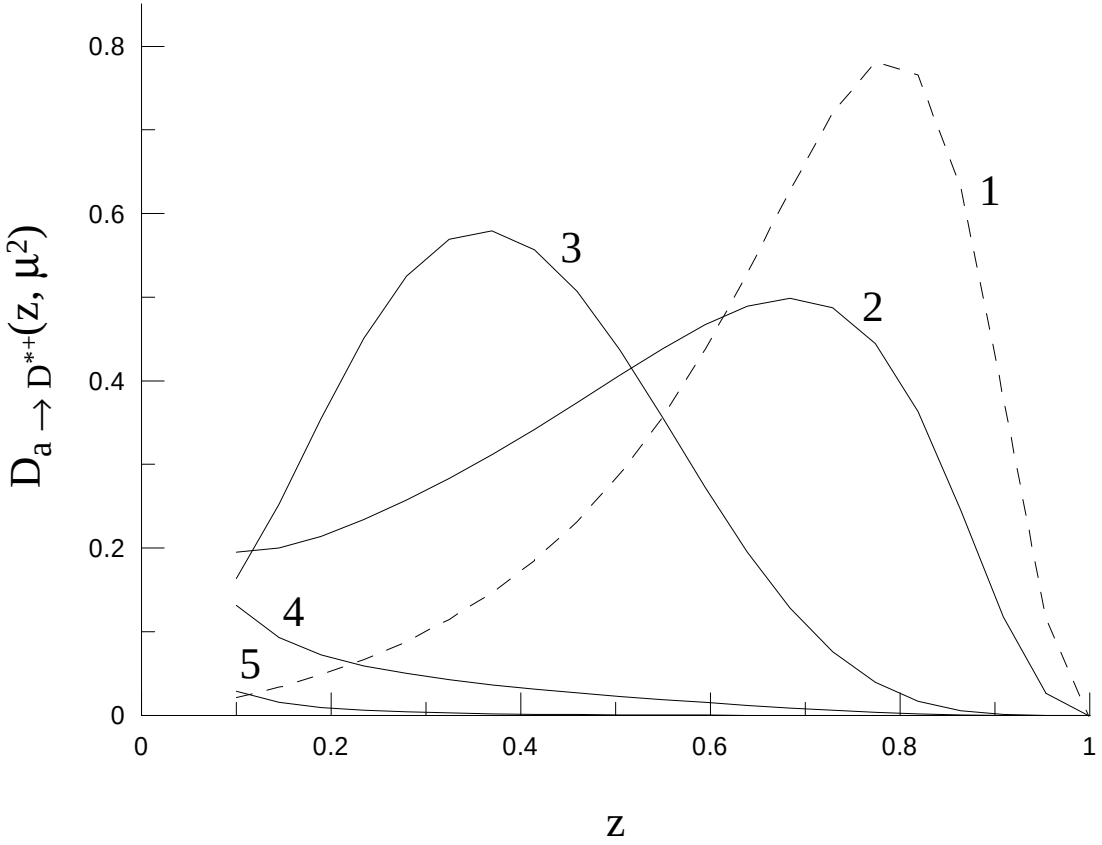

The fragmentation function $D_{a\to D}(z,\mu^2)$ by Kniehl and Kramer at the $\mu^2=\mu_0^2=2.25$ GeV^2 (curve 1) and $\mu^2=100$ GeV^2 (curves 2 – 5). Curves 1 and 2 for c-quark, curve 3 for b-quark, curve 4 for gluon and curve 5 for u-quark fragmentation into $D^{\star+}$. All input parameters for the D-mesons are taken from paper by B. Kniehl and G. Kramer, PRD74,037502(2006)

B- and D-meson production at the Tevatron and at the LHC

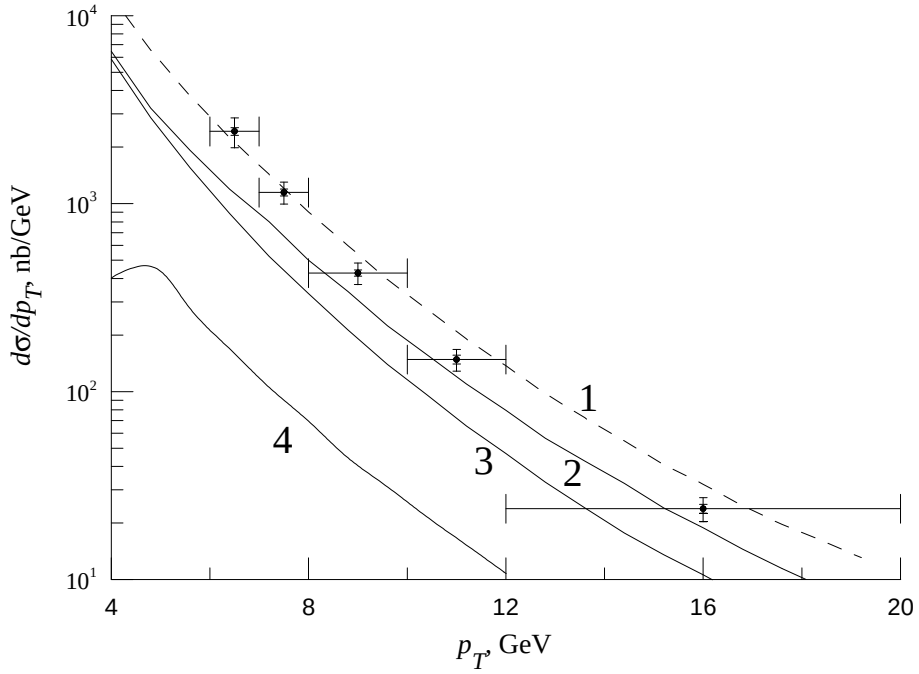

p_T spectrum of $D^{\star +}$-mesons. Curve 1 is the sum of all contributions, curve 2 is the $c-$quark contribution, curve 3 is the gluon contribution, curve 4 is the $b-$quark contribution. The CDF data are from Tevatron at $\sqrt{S} = 1.96$ TeV and $|y| < 1$.

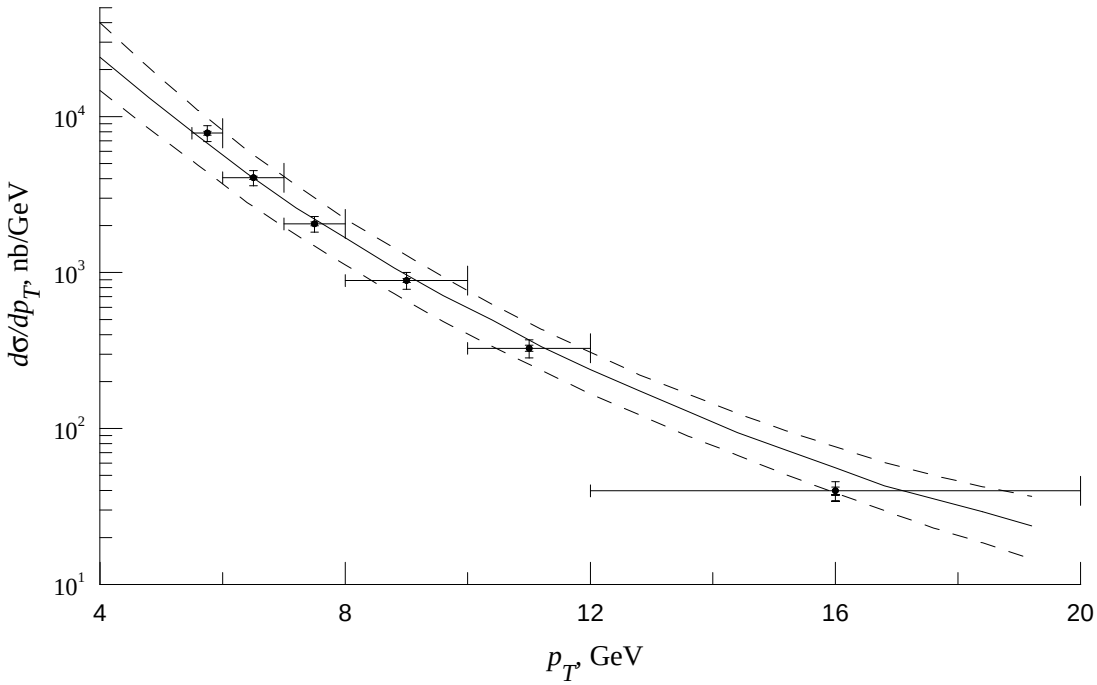

p_T spectra of D^0-mesons at $\sqrt{S} = 1.96$ TeV and $|y| < 1$ compared with CDF II data from Tevatron. Upper dashed curve corresponds $\mu = M_T/2$, lower dashed curve – $\mu = 2M_T$, solid line - $\mu = M_T$.

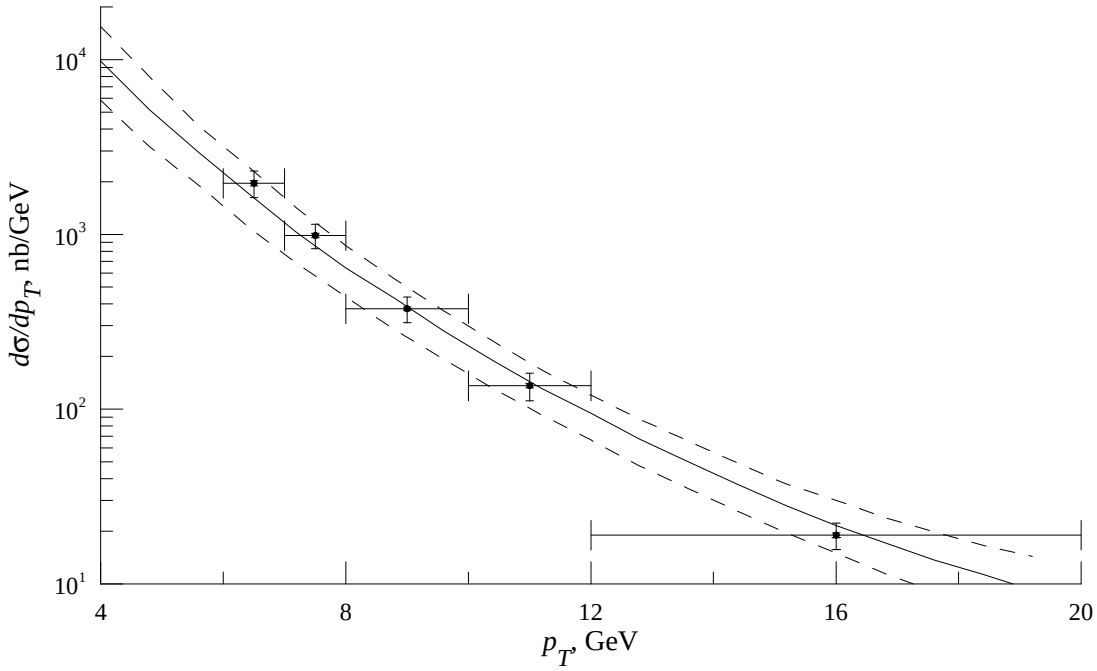

p_T spectra of D^+-mesons at $\sqrt{S} = 1.96$ TeV and $|y| < 1$ compared with CDF II data from Tevatron. Upper dashed curve corresponds $\mu = M_T/2$, lower dashed curve – $\mu = 2M_T$, solid line - $\mu = M_T$.

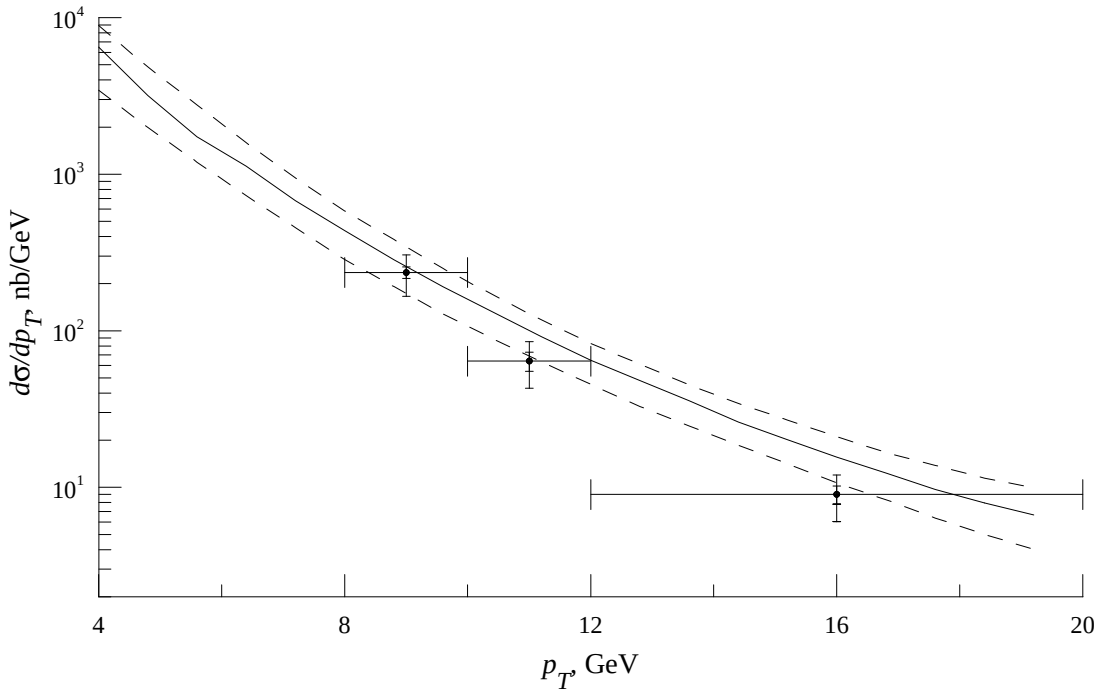

p_T spectra of D_s-mesons at $\sqrt{S} = 1.96$ TeV and $|y| < 1$ compared with CDF II data from Tevatron. Upper dashed curve corresponds $\mu = M_T/2$, lower dashed curve – $\mu = 2M_T$, solid line - $\mu = M_T$.

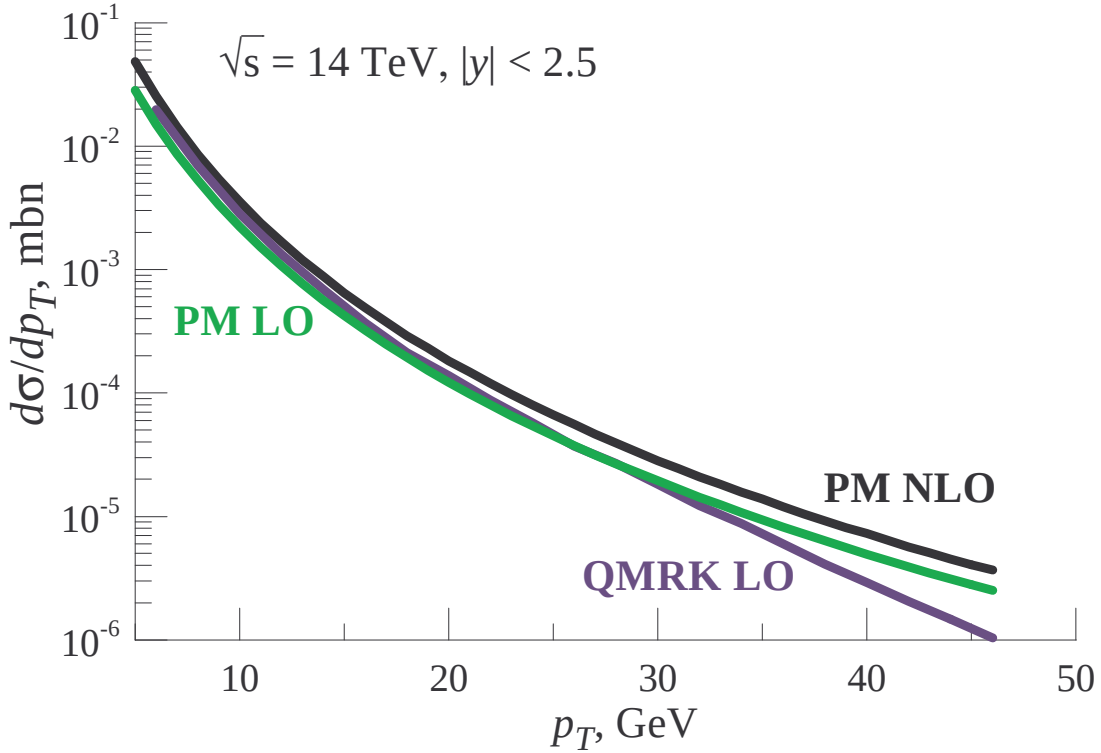

p_T spectra of $D^{\star +}$ mesons at $\sqrt{S} = 14$ TeV and $|y| < 2.5$.

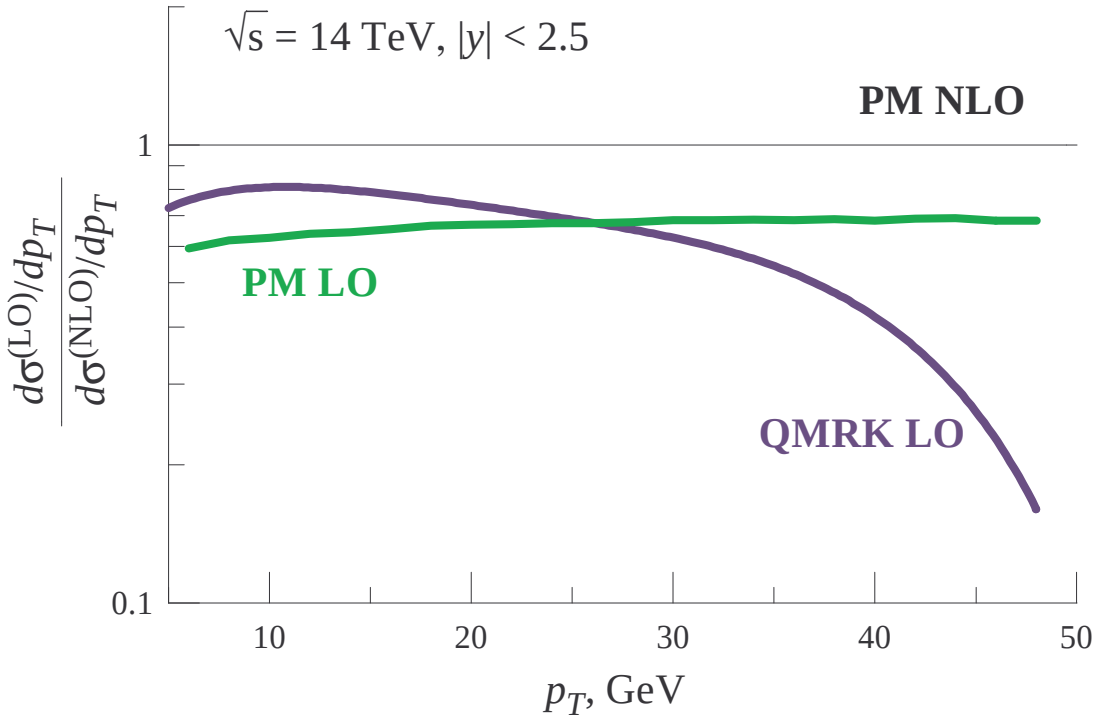

p_T spectra of $D^{\star +}$ mesons at $\sqrt{S} = 14$ TeV and $|y| < 2.5$.

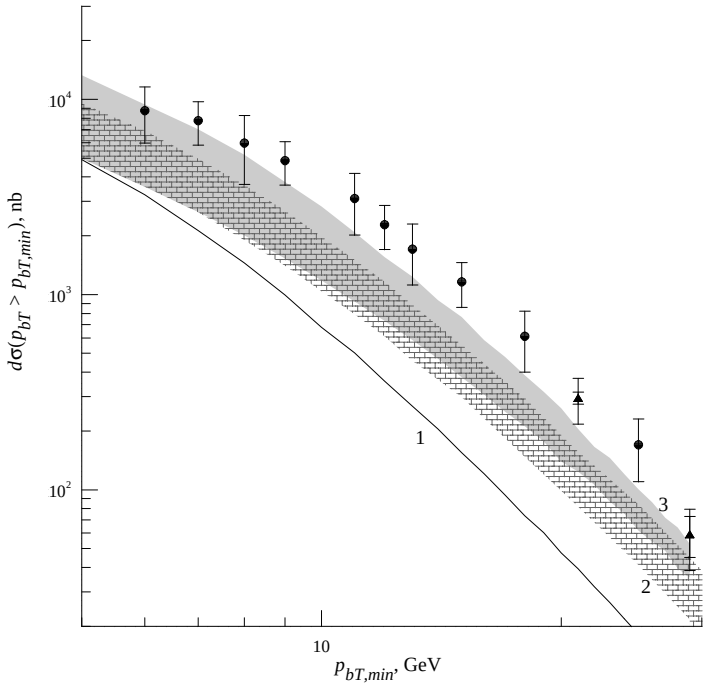

Figure 2: Theoretical results of b-quark hadroproduction at $\sqrt{S} = 1.8$ GeV and $|y| < 1$ compared with D0 CDF data from Tevatron. Curve 1 — collinear parton model prediction at LO, 2 — collinear parton model prediction at NLO , 3 — LO predictions in QMRK.

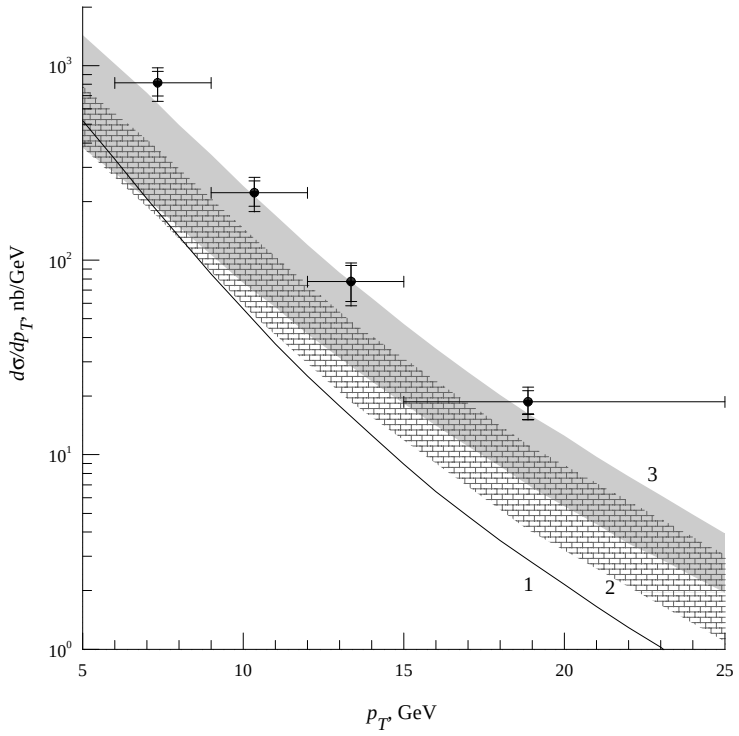

Figure 3: Theoretical results of B^+-meson hadroproduction at $\sqrt{S} = 1.8$ GeV and $|y| < 1$ compared with CDF data from Tevatron . Curve 1 — collinear parton model prediction at LO, 2 — collinear parton model prediction at NLO , 3 — LO predictions in QMRK.

NRQCD formalism

The factorization hypothesis of nonrelativistic QCD (NRQCD) assumes the separation of the effects of long and short distances in heavy-quarkonium production.

NRQCD is organized as a perturbative expansion in two small parameters, the strong-coupling constant α_s and the relative velocity v of the heavy quarks.

In the framework of the NRQCD factorization approach, the cross section of heavy-quarkonium production in a partonic subprocess $a + b \to \mathcal{H} + X$ may be presented as a sum of terms in which the effects of long and short distances are factorized as

$$d\hat{\sigma}(a + b \to \mathcal{H} + X) = \sum_n d\hat{\sigma}(a + b \to Q\bar{Q}[n] + X)\langle \mathcal{O}^{\mathcal{H}}[n]\rangle, \quad (24)$$

The cross section $d\hat{\sigma}(a + b \to Q\bar{Q}[n] + X)$ can be calculated in perturbative QCD as an expansion in α_s using the non-relativistic approximation for the relative motion of the heavy quarks in the $Q\bar{Q}$ pair.

The non-perturbative transition of the $Q\bar{Q}$ pair into the physical quarkonium state $\mathcal{H}$ is described by the NMEs $\langle \mathcal{O}^{\mathcal{H}}[n]\rangle$, which can be extracted from experimental data.

To leading order in v, we need to include the $Q\bar{Q}$ Fock states $n = {}^3S_1^{(1)}, {}^3S_1^{(8)}, {}^1S_0^{(8)}, {}^3P_J^{(8)}$ if $\mathcal{H} = \Upsilon(nS), \psi(nS)$, and $n = {}^3P_J^{(1)}, {}^3S_1^{(8)}$ if $\mathcal{H} = \chi_{bJ,cJ}(nP)$, where $J = 0, 1$ or 2. Their NMEs satisfy the multiplicity relations

$$\begin{aligned}
\langle \mathcal{O}^{\Upsilon(nS)}[{}^3P_J^{(8)}]\rangle &= (2J+1)\langle \mathcal{O}^{\Upsilon(nS)}[{}^3P_0^{(8)}]\rangle, \\
\langle \mathcal{O}^{\chi_{bJ}(nP)}[{}^3P_J^{(1)}]\rangle &= (2J+1)\langle \mathcal{O}^{\chi_{b0}(nP)}[{}^3P_0^{(1)}]\rangle, \\
\langle \mathcal{O}^{\chi_{bJ}(nP)}[{}^3S_1^{(8)}]\rangle &= (2J+1)\langle \mathcal{O}^{\chi_{b0}(nP)}[{}^3S_1^{(8)}]\rangle,
\end{aligned}$$

which follow to LO in v from heavy-quark spin symmetry.

$$\langle \mathcal{O}^{\Upsilon(nS)}[{}^3S_1^{(1)}]\rangle = 2N_c(2J+1)|\Psi_n(0)|^2, \tag{25}$$

where $N_c = 3$ and $J = 1$.

$$\langle \mathcal{O}^{\chi_{bJ}(nP)}[{}^3P_J^{(1)}]\rangle = 2N_c(2J+1)|\Psi'(0)|^2. \tag{26}$$

$$d\hat{\sigma}(a+b \to Q\bar{Q}[^{2S+1}L_J^{(1,8)}] \to \mathcal{H}) =$$
$$d\hat{\sigma}(a+b \to Q\bar{Q}[^{2S+1}L_J^{(1,8)}]) \frac{\langle \mathcal{O}^{\mathcal{H}}[^{2S+1}L_J^{(1,8)}]\rangle}{N_{\rm col} N_{\rm pol}}$$

where $N_{\rm col} = 2N_c$ for the color-singlet state, $N_{\rm col} = N_c^2 - 1$ for the color-octet state, and $N_{\rm pol} = 2J + 1$.

The production amplitude

$$\mathcal{A}(a+b \to Q\bar{Q}[^{2S+1}L_J^{(1,8)}])$$

can be obtained from the one for an unspecified $Q\bar{Q}$ state, $\mathcal{A}(a+b \to Q\bar{Q})$, by the application of appropriate projectors.

The projectors on the spin-0 and spin-1 states read:

$$\Pi_0 = \frac{1}{\sqrt{8m^3}}\left(\frac{\hat{p}}{2}-\hat{q}-m\right)\gamma_5\left(\frac{\hat{p}}{2}+\hat{q}+m\right),$$

$$\Pi_1^\alpha = \frac{1}{\sqrt{8m^3}}\left(\frac{\hat{p}}{2}-\hat{q}-m\right)\gamma^\alpha\left(\frac{\hat{p}}{2}+\hat{q}+m\right)$$

The projection operators on the color-singlet and color-octet states read:

$$C_1 = \frac{\delta_{ij}}{\sqrt{N_c}} \text{ and } C_8 = \sqrt{2}T^c_{ij}. \tag{27}$$

To obtain the projection on the state with orbital-angular-momentum quantum number L, we need take L times the derivative with respect to q and then put $q = 0$.

$$\mathcal{A}(a + b \to Q\bar{Q}[^1S_0^{(1,8)}]) =$$
$$= \mathrm{Tr}\left[C_{1,8}\Pi_0 \mathcal{A}(a + b \to Q\bar{Q})\right]|_{q=0},$$
$$\mathcal{A}(a + b \to Q\bar{Q}[^3S_1^{(1,8)}]) =$$
$$= \mathrm{Tr}\left[C_{1,8}\Pi_1^{\alpha} \mathcal{A}(a + b \to Q\bar{Q})\varepsilon_{\alpha}(p)\right]|_{q=0},$$
$$\mathcal{A}(a + b \to Q\bar{Q}[^3P_J^{(1,8)}]) =$$
$$= \frac{d}{dq_{\beta}}\mathrm{Tr}\left[C_{1,8}\Pi_1^{\alpha} \mathcal{A}(a + b \to Q\bar{Q})\varepsilon_{\alpha\beta}(p)\right]|_{q=0}$$

Heavy quarkonium production
by reggeized gluons

In this section, we obtain the squared amplitudes for inclusive quarkonium production via the fusion of two reggeized gluons in the framework of the NRQCD. We work at LO in α_s and v and consider the following partonic subprocessses:

$$\begin{aligned} R+R &\to \mathcal{H}[{}^3P_J^{(1)}, {}^3S_1^{(8)}, {}^1S_0^{(8)}, {}^3P_J^{(8)}], \\ R+R &\to \mathcal{H}[{}^3S_1^{(1)}] + g, \end{aligned}$$

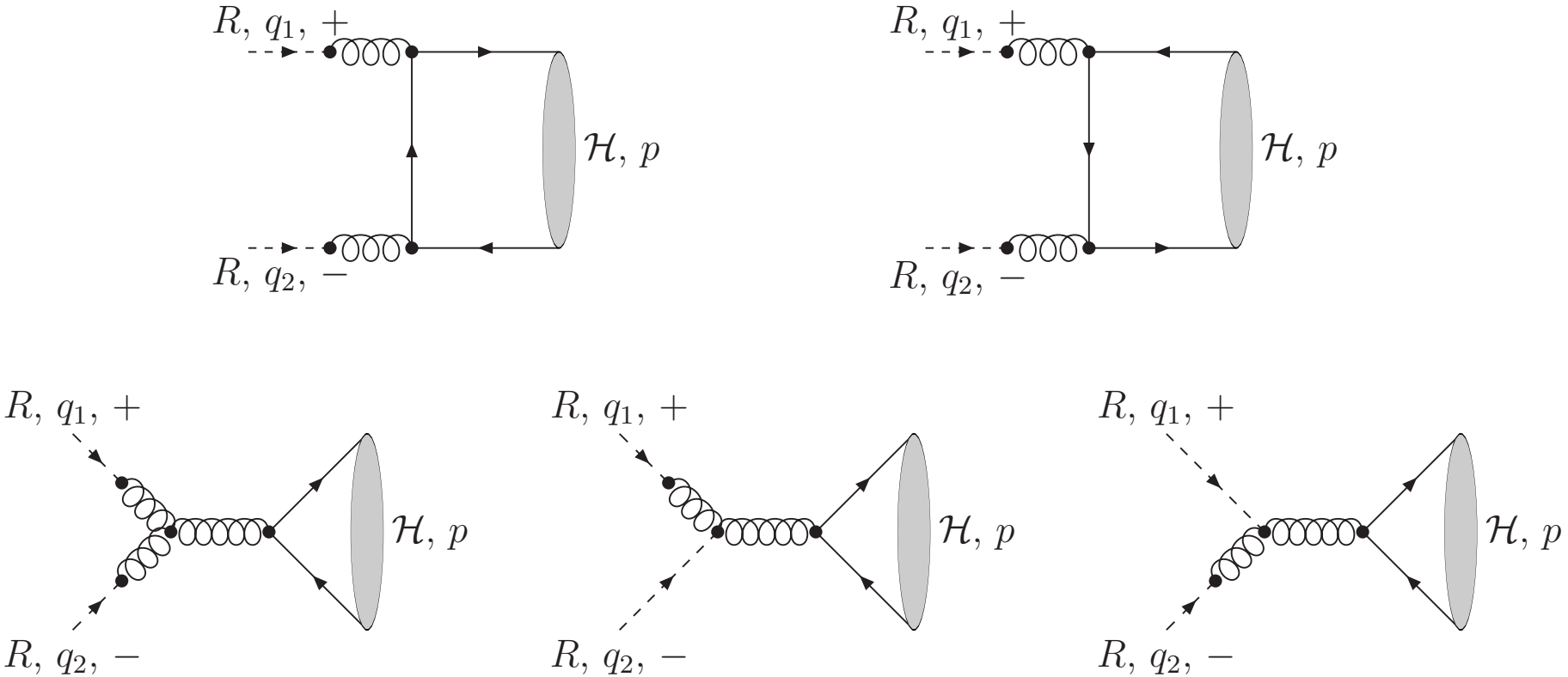

Feynman diagrams for subprocesses $R^+R^- \to \mathcal{H}$.

We have obtained

$$\overline{|\mathcal{A}(R+R\to\mathcal{H}[^3P_0^{(1)}])|^2} = \frac{8}{3}\pi^2\alpha_s^2\frac{\langle\mathcal{O}^{\mathcal{H}}[^3P_0^{(1)}]\rangle}{M^5}F^{[^3P_0]}(t_1,t_2,\varphi),$$

$$\overline{|\mathcal{A}(R+R\to\mathcal{H}[^3P_1^{(1)}])|^2} = \frac{16}{3}\pi^2\alpha_s^2\frac{\langle\mathcal{O}^{\mathcal{H}}[^3P_1^{(1)}]\rangle}{M^5}F^{[^3P_1]}(t_1,t_2,\varphi),$$

$$\overline{|\mathcal{A}(R+R\to\mathcal{H}[^3P_2^{(1)}])|^2} = \frac{32}{45}\pi^2\alpha_s^2\frac{\langle\mathcal{O}^{\mathcal{H}}[^3P_2^{(1)}]\rangle}{M^5}F^{[^3P_2]}(t_1,t_2,\varphi),$$

$$\overline{|\mathcal{A}(R+R\to\mathcal{H}[^3S_1^{(8)}])|^2} = \frac{1}{2}\pi^2\alpha_s^2\frac{\langle\mathcal{O}^{\mathcal{H}}[^3S_1^{(8)}]\rangle}{M^3}F^{[^3S_1]}(t_1,t_2,\varphi),$$

$$\overline{|\mathcal{A}(R+R\to\mathcal{H}[^1S_0^{(8)}])|^2} = \frac{5}{12}\pi^2\alpha_s^2\frac{\langle\mathcal{O}^{\mathcal{H}}[^1S_0^{(8)}]\rangle}{M^3}F^{[^1S_0]}(t_1,t_2,\varphi),$$

$$\overline{|\mathcal{A}(R+R\to\mathcal{H}[^3P_0^{(8)}])|^2} = 5\pi^2\alpha_s^2\frac{\langle\mathcal{O}^{\mathcal{H}}[^3P_0^{(8)}]\rangle}{M^5}F^{[^3P_0]}(t_1,t_2,\varphi),$$

$$\overline{|\mathcal{A}(R+R\to\mathcal{H}[^3P_1^{(8)}])|^2} = 10\pi^2\alpha_s^2\frac{\langle\mathcal{O}^{\mathcal{H}}[^3P_1^{(8)}]\rangle}{M^5}F^{[^3P_1]}(t_1,t_2,\varphi),$$

$$\overline{|\mathcal{A}(R+R\to\mathcal{H}[^3P_2^{(8)}])|^2} = \frac{4}{3}\pi^2\alpha_s^2\frac{\langle\mathcal{O}^{\mathcal{H}}[^3P_2^{(8)}]\rangle}{M^5}F^{[^3P_2]}(t_1,t_2,\varphi)$$

$$
\begin{aligned}
F^{[^3S_1]}(t_1,t_2,\varphi) &= \frac{16t_1t_2}{(M^2+t_1+t_2)^2(M^2+|\mathbf{p}_T|^2)}\big[(t_1+t_2)^2+ \\
&\quad +M^2\big(t_1+t_2-2\sqrt{t_1t_2}\cos\varphi\big)\big], \\
F^{[^1S_0]}(t_1,t_2,\varphi) &= \frac{32M^2t_1t_2\sin^2\varphi}{(M^2+t_1+t_2)^2}, \\
F^{[^3P_0]}(t_1,t_2,\varphi) &= \frac{32M^2t_1t_2}{9(M^2+t_1+t_2)^4}\big[(3M^2+t_1+t_2)\cos\varphi+ \\
&\quad +2\sqrt{t_1t_2}\big]^2, \\
F^{[^3P_1]}(t_1,t_2,\varphi) &= \frac{32M^2t_1t_2}{9(M^2+t_1+t_2)^4}\big[(t_1+t_2)^2\sin^2\varphi+ \\
&\quad +M^2\big(t_1+t_2-2\sqrt{t_1t_2}\cos\varphi\big)\big], \\
F^{[^3P_2]}(t_1,t_2,\varphi) &= \frac{16M^2t_1t_2}{3(M^2+t_1+t_2)^4}\big[3M^4+3(t_1+t_2)M^2+ \\
&\quad +(t_1+t_2)^2\cos^2\varphi+4t_1t_2+ \\
&\quad +2\sqrt{t_1t_2}\,\big[3M^2+2(t_1+t_2)\big]\cos\varphi\big],
\end{aligned}
$$

Here $\mathbf{p}_T = \mathbf{q}_{1T} + \mathbf{q}_{2T}$, $t_{1,2} = |\mathbf{q}_{1,2T}|^2$, and $\varphi = \varphi_1 - \varphi_2$ is the angle enclosed between $\mathbf{q}_{1T}$ and $\mathbf{q}_{2T}$, so that

$$|\mathbf{p}_T|^2 = t_1 + t_2 + 2\sqrt{t_1 t_2}\cos\varphi$$

$$\overline{|\mathcal{A}(g+g \to \mathcal{H}[^{2S+1}L_J^{(1,8)}]|^2} = \lim_{t_1,t_2\to 0}\int_0^{2\pi}\frac{d\varphi_1}{2\pi}\int_0^{2\pi}\frac{d\varphi_2}{2\pi}\mathcal{N}\times\overline{|\mathcal{A}(R+R \to \mathcal{H}[^{2S+1}L_J^{(1,8)}]|^2}.$$

In this way, we recover the well-known results:

$$\overline{|\mathcal{A}(g+g\to\mathcal{H}[^3P_0^{(1)}]|^2} = \frac{8}{3}\pi^2\alpha_s^2\frac{\langle\mathcal{O}^{\mathcal{H}}[^3P_0^{(8)}]\rangle}{M^3},$$

$$\overline{|\mathcal{A}(g+g\to\mathcal{H}[^3P_1^{(1)}]|^2} = 0,$$

$$\overline{|\mathcal{A}(g+g\to\mathcal{H}[^3P_2^{(1)}]|^2} = \frac{32}{45}\pi^2\alpha_s^2\frac{\langle\mathcal{O}^{\mathcal{H}}[^3P_2^{(8)}]\rangle}{M^3},$$

$$\overline{|\mathcal{A}(g+g\to\mathcal{H}[^3S_1^{(8)}]|^2} = 0,$$

$$\overline{|\mathcal{A}(g+g\to\mathcal{H}[^1S_0^{(8)}]|^2} = \frac{5}{12}\pi^2\alpha_s^2\frac{\langle\mathcal{O}^{\mathcal{H}}[^1S_0^{(8)}]\rangle}{M},$$

$$\overline{|\mathcal{A}(g+g\to\mathcal{H}[^3P_0^{(8)}]|^2} = 5\pi^2\alpha_s^2\frac{\langle\mathcal{O}^{\mathcal{H}}[^3P_0^{(8)}]\rangle}{M^3},$$

$$\overline{|\mathcal{A}(g+g\to\mathcal{H}[^3P_1^{(8)}]|^2} = 0,$$

$$\overline{|\mathcal{A}(g+g\to\mathcal{H}[^3P_2^{(8)}]|^2} = \frac{4}{3}\pi^2\alpha_s^2\frac{\langle\mathcal{O}^{\mathcal{H}}[^3P_2^{(8)}]\rangle}{M^3}.$$

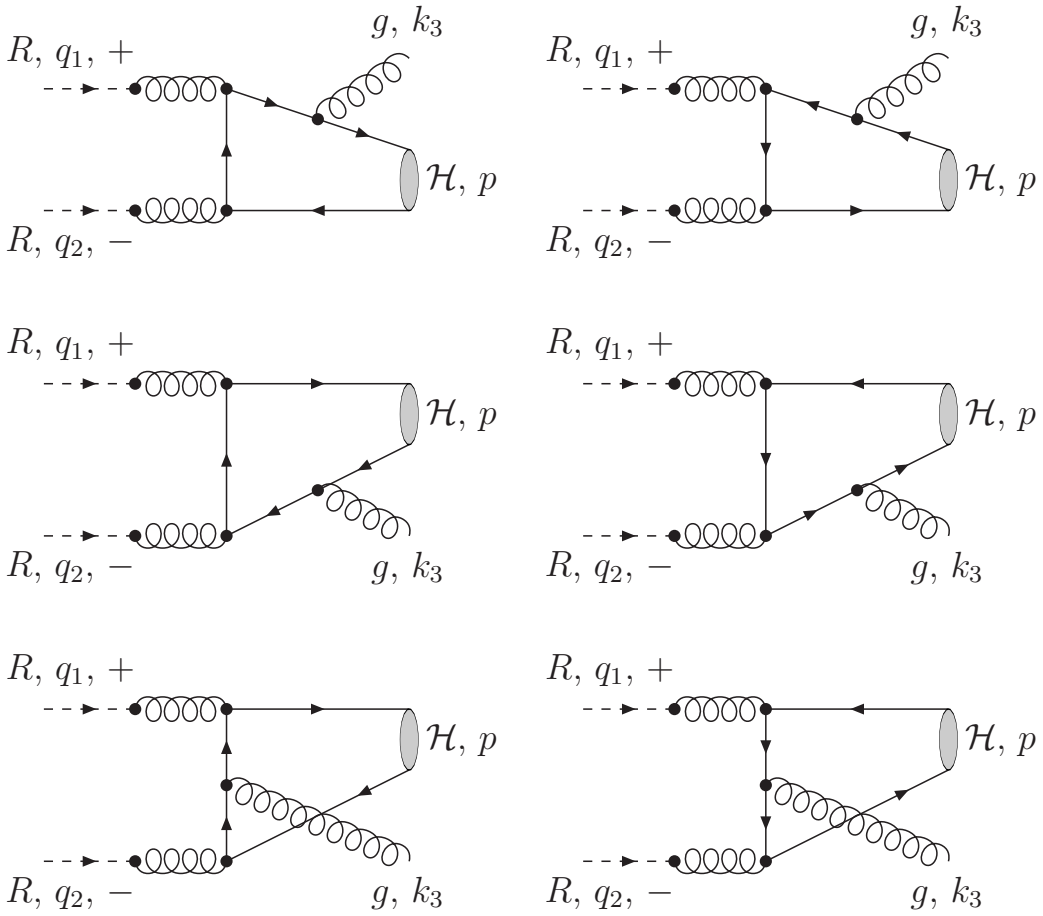

Feynman diagrams for subprocesses $R^+ + R^- \to \mathcal{H}[^3S_1^{(1)}]\mathrm{g}$.

Heavy quarkonium production
at the Tevatron

Nowadays Tevatron CDF data incorporate p_T-spectra for prompt $\Upsilon(1S, 2S, 3S)$ at the $\sqrt{S} = 1.8$ TeV and for prompt $\Upsilon(1S)$ in the different intervals of rapidity at the $\sqrt{S} = 1.96$ TeV; for direct J/ψ, for J/ψ from ψ' decays, for J/ψ from χ_{cJ} decays at the $\sqrt{S} = 1.8$ TeV; for prompt J/ψ at the $\sqrt{S} = 1.96$ TeV.

$$\sigma^{prompt}(J/\psi) = \sigma^{direct}(J/\psi) + \sigma(\psi' \to J/\psi) +$$
$$+\sigma(\chi_{cJ} \to J/\psi) + \sigma(\psi' \to \chi_{cJ} \to J/\psi)$$

In contrast to previous analysis in the collinear parton model we perform a joint fit to the run-I and run-II CDF data for all p_T, including the region of small p_T, to obtain the color-octet NMEs for $\psi(nS), \Upsilon(nS)$ and $\chi_{cJ}(1P), \chi_{bJ}(nP)$ using three different unintegrated gluon distribution functions. Our calculations are based on exact analytical expressions for the relevant squared amplitudes, obtained in the QMRK approach.

The rapidity and pseudorapidity of a heavy quarkonium state with four-momentum $p_\mu = (p_0, \mathbf{p}_T, p_3)$ are given by

$$y = \frac{1}{2} \ln \frac{p_0 + p_3}{p_0 - p_3}, \quad \eta = \frac{1}{2} \ln \frac{|\mathbf{p}| + p_3}{|\mathbf{p}| - p_3},$$

respectively. We use also following variables

$$\xi_1 = \frac{p_0 + p_3}{2E_1}, \qquad \xi_2 = \frac{p_0 - p_3}{2E_2}.$$

In the case of the $2 \to 1$ subprocesses, we obtain

$$\frac{d\sigma(p+p \to \mathcal{H}+X)}{d|\mathbf{p}_T|dy} = \frac{|\mathbf{p}_T|}{8}\int \frac{d^2\mathbf{q}_{1T}}{|\mathbf{q}_{1T}|^2}\int \frac{d^2\mathbf{q}_{2T}}{|\mathbf{q}_{2T}|^2}\Phi(\xi_1,|\mathbf{q}_{1T}|^2,\mu^2)\times$$
$$\times\Phi(\xi_2,|\mathbf{q}_{2T}|^2,\mu^2)\delta(\mathbf{q}_{1T}+\mathbf{q}_{1T}-\mathbf{p}_T)\overline{|\mathcal{A}(R+R\to\mathcal{H})|^2}.$$

For the $2 \to 2$ subprocess, we have

$$\frac{d\sigma(p+p \to \mathcal{H}+X)}{d|\mathbf{p}_T|dy} = \frac{|\mathbf{p}_T|}{128\pi^3}\int \frac{d^2\mathbf{q}_{1T}}{|\mathbf{q}_{1T}|^2}\int \frac{d^2\mathbf{q}_{2T}}{|\mathbf{q}_{2T}|^2}\int \frac{dx_2}{x_2-\xi_2}\times$$
$$\times\Phi(x_1,|\mathbf{q}_{1T}|^2,\mu^2)\Phi(x_2,|\mathbf{q}_{2T}|^2,\mu^2)\overline{|\mathcal{A}(R+R\to\mathcal{H}+g)|^2},$$

where

$$x_1 = \frac{1}{(x_2-\xi_2)S}\Big((\mathbf{q}_{1T}+\mathbf{q}_{2T}-\mathbf{p}_T)^2 - M^2 - |\mathbf{p}_T|^2 + x_2\xi_1 S\Big).$$

In previous fit of CDF data were used for the region of large $|\mathbf{p}_T| > 8(4)$ GeV only, and the linear combination

$$M_r^{\mathcal{H}} = \langle \mathcal{O}^{\mathcal{H}}[^1S_0^{(8)}] \rangle + \frac{r}{m_Q^2} \langle \mathcal{O}^{\mathcal{H}}[^3P_0^{(8)}] \rangle \tag{28}$$

was fixed because it was unfeasible to separate the contributions proportional to $\langle \mathcal{O}^{\mathcal{H}}[^1S_0^{(8)}] \rangle$ and $\langle \mathcal{O}^{\mathcal{H}}[^3P_0^{(8)}] \rangle$.

By contrast, QMRK fit allow us to determine $\langle \mathcal{O}^{\mathcal{H}}[^1S_0^{(8)}] \rangle$ and $\langle \mathcal{O}^{\mathcal{H}}[^3P_0^{(8)}] \rangle$ separately, which is due to the different $|\mathbf{p}_T|$ dependence of the respective contributions for $|\mathbf{p}_T| < 8(4)$ GeV.

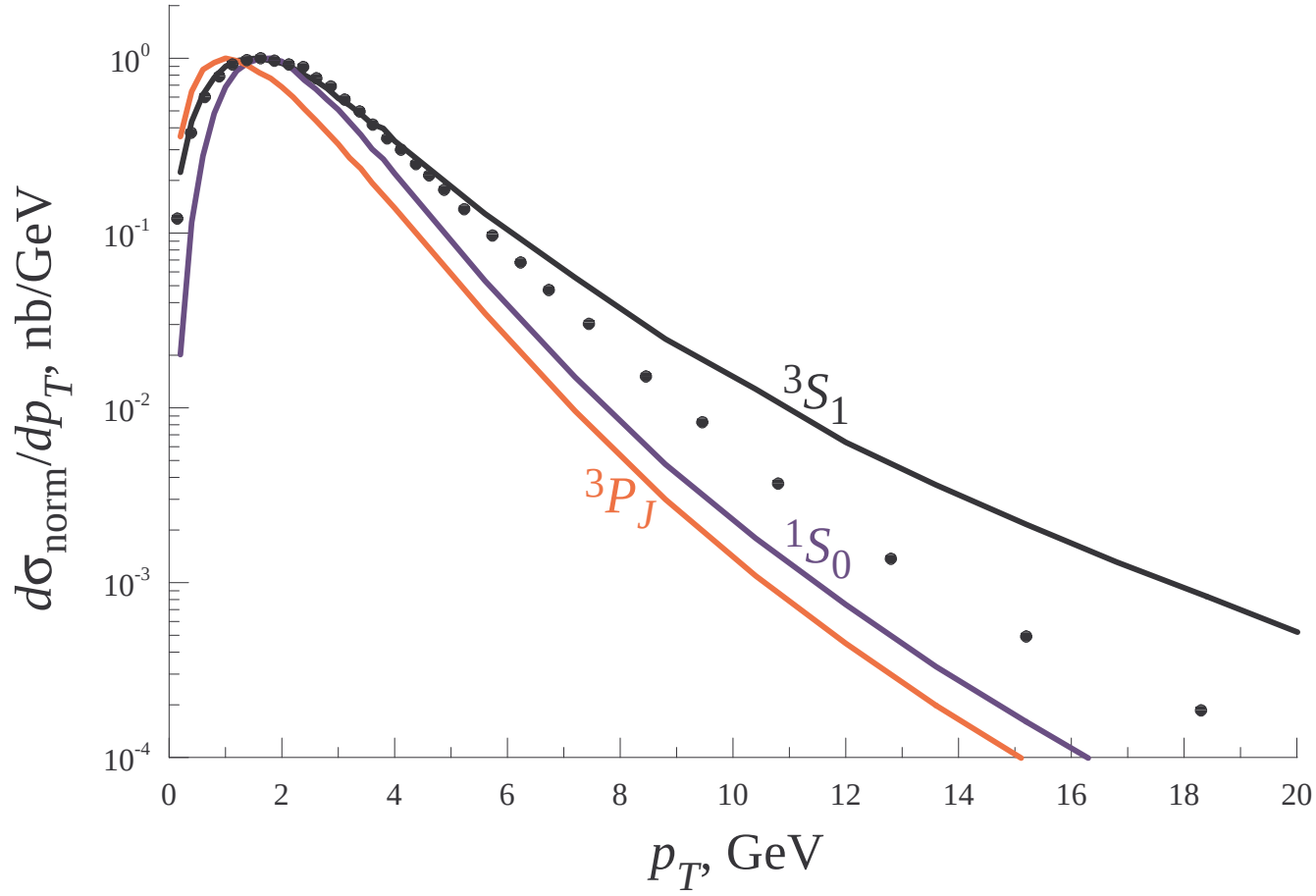

Contributions to the p_T distribution of direct $\Upsilon(1S)$ hadroproduction in $p\bar{p}$ scattering with $\sqrt{S} = 1.8$ TeV and $|y| < 0.4$ from the relevant color-octet states. All distributions are normalized on unit in their peak values.

Table: NMEs for J/ψ, ψ' and χ_{cJ}

NME	PM	Fit JB	Fit JS	Fit KMR
$\langle \mathcal{O}^{J/\psi}[^3S_1^{(1)}]\rangle/\mathrm{GeV}^3$	1.3	1.3	1.3	1.3
$\langle \mathcal{O}^{J/\psi}[^3S_1^{(8)}]\rangle/\mathrm{GeV}^3$	$4.4\cdot10^{-3}$	$1.5\cdot10^{-3}$	$6.1\cdot10^{-3}$	$2.7\cdot10^{-3}$
$\langle \mathcal{O}^{J/\psi}[^1S_0^{(8)}]\rangle/\mathrm{GeV}^3$	$4.3\cdot10^{-2}$	$6.6\cdot10^{-3}$	$9.0\cdot10^{-3}$	$1.4\cdot10^{-2}$
$\langle \mathcal{O}^{J/\psi}[^3P_0^{(8)}]\rangle/\mathrm{GeV}^5$	$2.8\cdot10^{-2}$	0	0	0
$\langle \mathcal{O}^{\psi'}[^3S_1^{(1)}]\rangle/\mathrm{GeV}^3$	$6.5\cdot10^{-1}$	$6.5\cdot10^{-1}$	$6.5\cdot10^{-1}$	$6.5\cdot10^{-1}$
$\langle \mathcal{O}^{\psi'}[^3S_1^{(8)}]\rangle/\mathrm{GeV}^3$	$4.2\cdot10^{-3}$	$3.0\cdot10^{-4}$	$1.5\cdot10^{-3}$	$8.3\cdot10^{-4}$
$\langle \mathcal{O}^{\psi'}[^1S_0^{(8)}]\rangle/\mathrm{GeV}^3$	$6.9\cdot10^{-3}$	0	0	0
$\langle \mathcal{O}^{\psi'}[^3P_0^{(8)}]\rangle/\mathrm{GeV}^5$	$3.9\cdot10^{-3}$	0	0	0
$\langle \mathcal{O}^{\chi_{c0}}[^3P_0^{(1)}]\rangle/\mathrm{GeV}^5$	$8.9\cdot10^{-2}$	$8.9\cdot10^{-2}$	$8.9\cdot10^{-2}$	$8.9\cdot10^{-2}$
$\langle \mathcal{O}^{\chi_{c0}}[^3S_1^{(8)}]\rangle/\mathrm{GeV}^3$	$4.4\cdot10^{-3}$	0	$2.2\cdot10^{-4}$	$4.7\cdot10^{-5}$
χ^2/d.o.f	–	2.2 (*)	4.1	3.0

$$\triangle L \approx \triangle S \approx 0$$

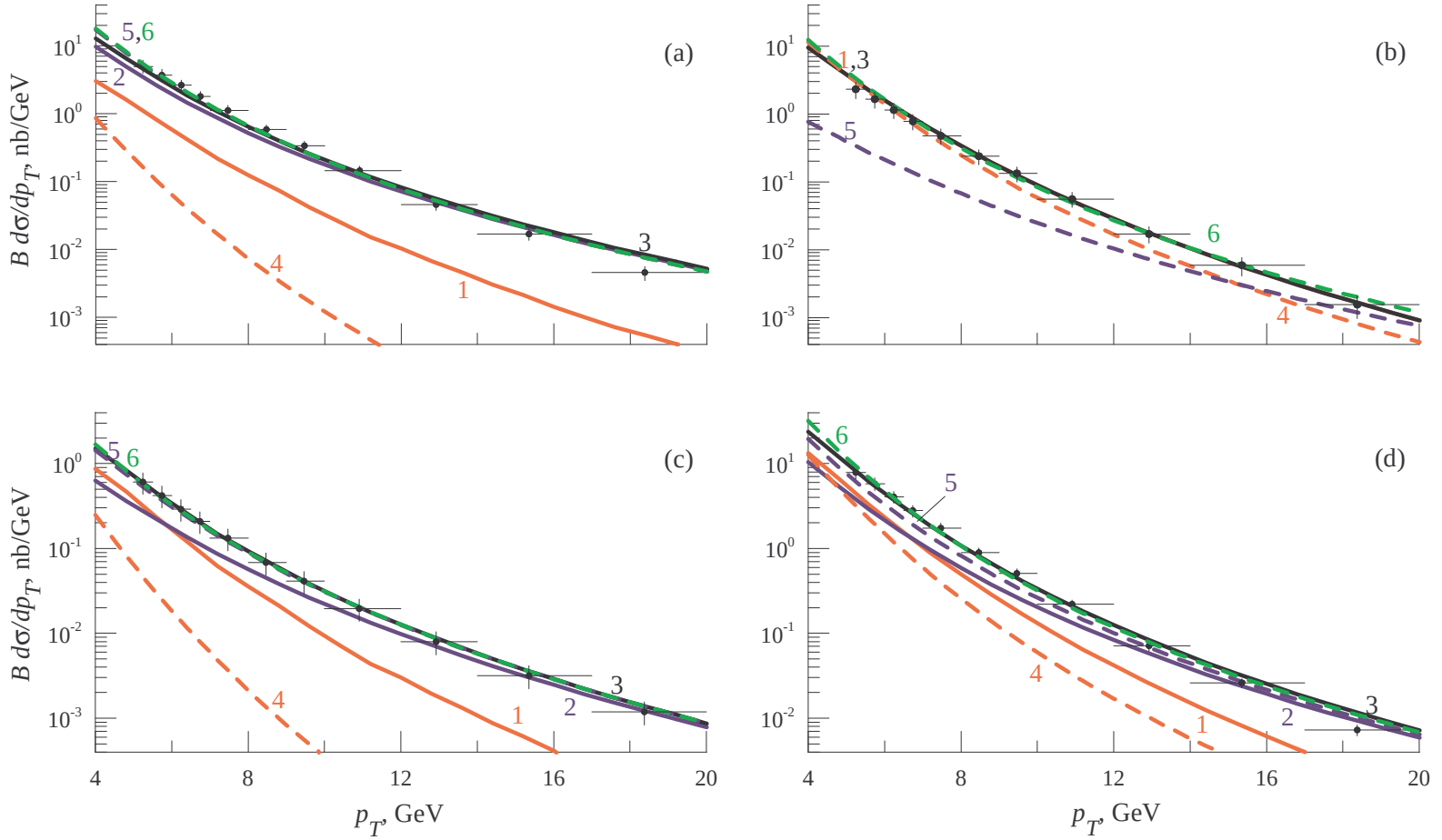

J/ψ at CDF (run I)

(a) direct, (b) χ_{cJ}-decays, (c) ψ'-decays, (d) prompt; solid lines - QMRK, dashed lines - PM; 1,4 - color-singlet, 2,5 - color-octet, 3,6 - total.

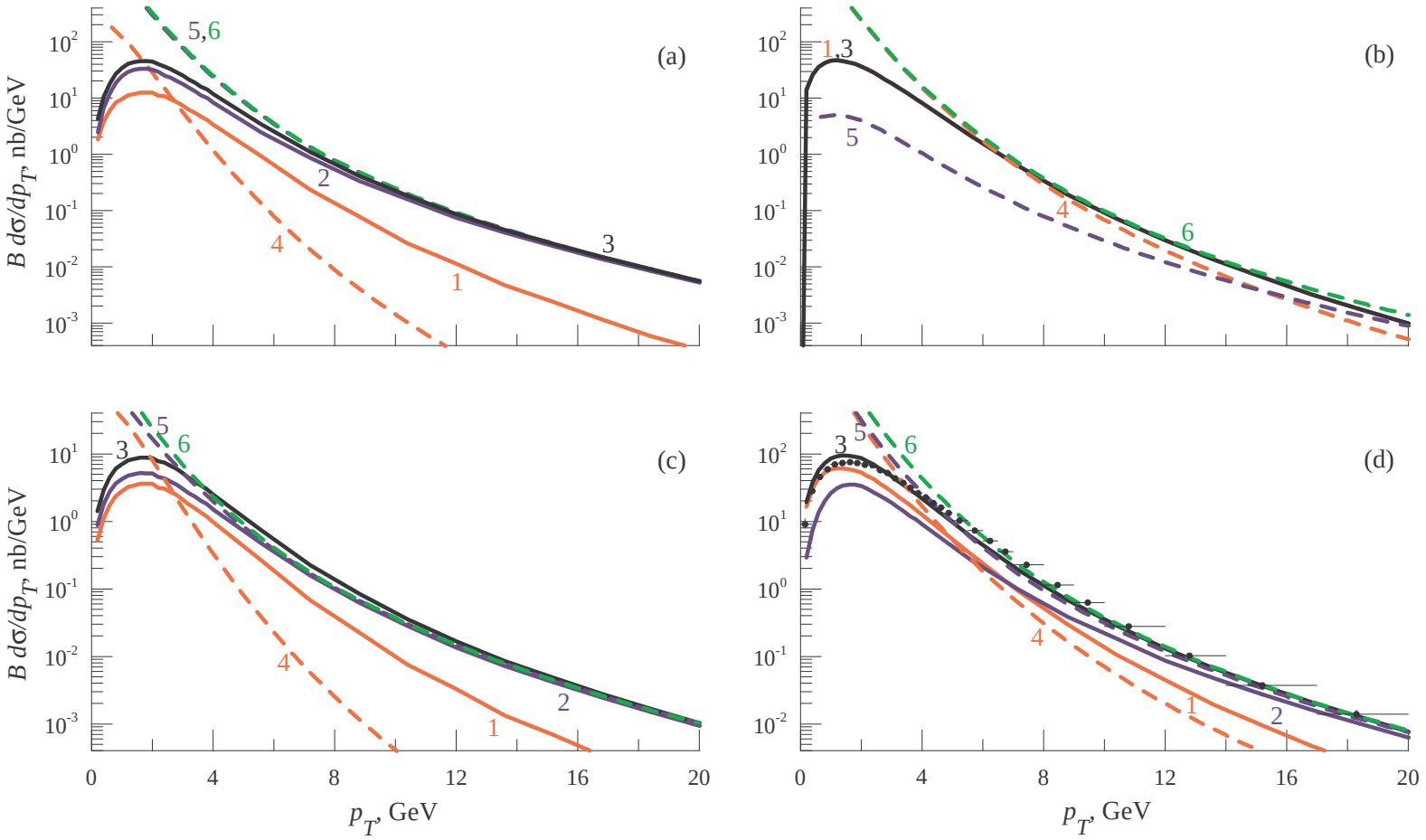

J/ψ at CDF (run II)

(a) direct, (b) χ_{cJ}-decays, (c) ψ'-decays, (d) prompt; solid lines - QMRK, dashed lines - PM; 1,4 - color-singlet, 2,5 - color-octet, 3,6 - total.

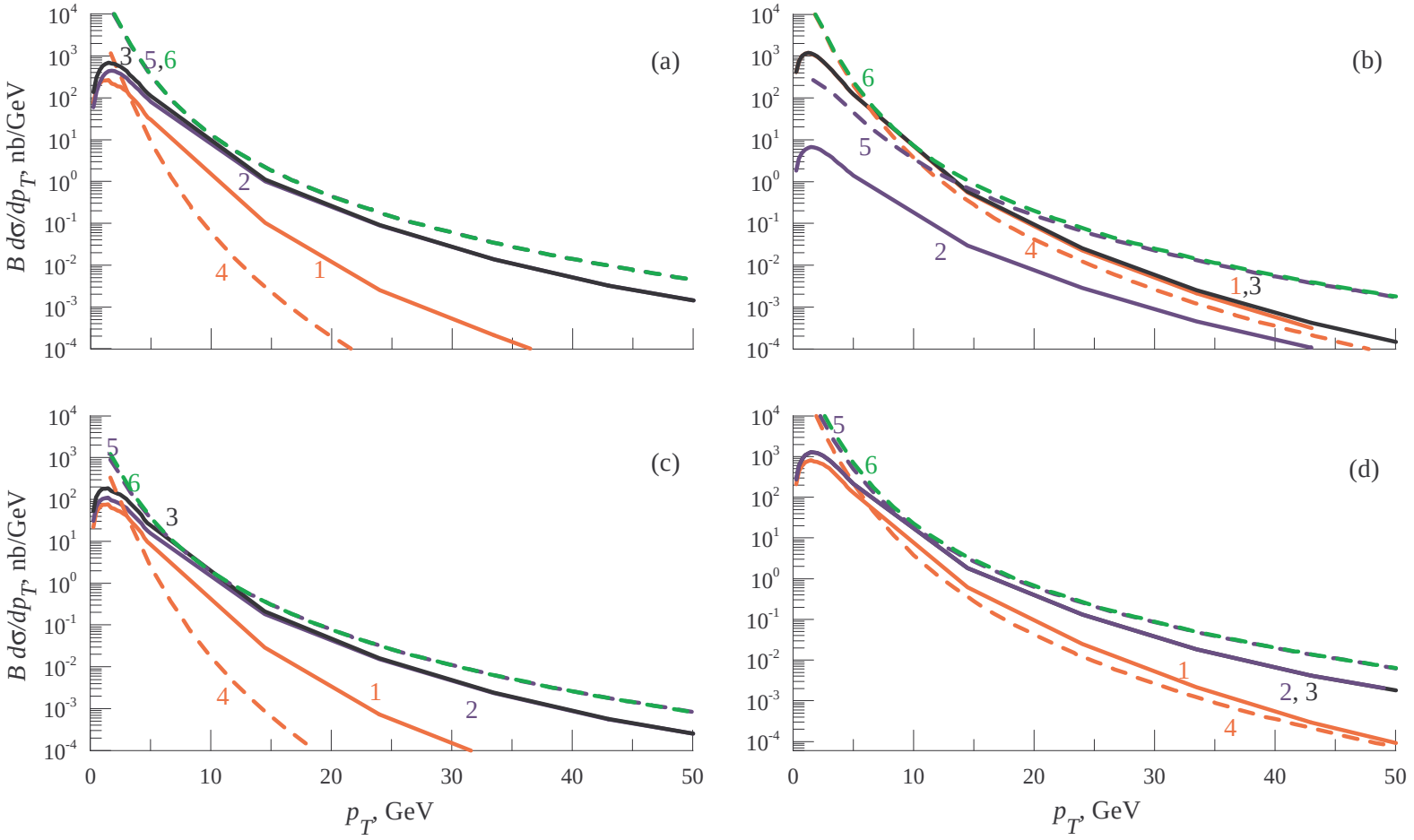

J/ψ at LHC, $|y| < 2.5$

(a) direct, (b) χ_{cJ}-decays, (c) ψ'-decays, (d) prompt; solid lines - QMRK, dashed lines - PM; 1,4 - color-singlet, 2,5 - color-octet, 3,6 - total.

Table: Inclusive branchings fractions for transitions between spin-triplet bottomonium states.

In\Out	$\Upsilon(3S)$	$\chi_{b2}(2P)$	$\chi_{b1}(2P)$	$\chi_{b0}(2P)$	$\Upsilon(2S)$	$\chi_{b2}(1P)$	$\chi_{b1}(1P)$	$\chi_{b0}(1P)$	$\Upsilon(1S)$
$\Upsilon(3S)$	1	0.114	0.113	0.054	0.106	0.007208	0.00742	0.004028	0.102171
$\chi_{b2}(2P)$	—	1	—	—	0.162	0.011016	0.01134	0.006156	0.129565
$\chi_{b1}(2P)$	—	—	1	—	0.21	0.01428	0.0147	0.00798	0.160917
$\chi_{b0}(2P)$	—	—	—	1	0.046	0.003128	0.00322	0.001748	0.0167195
$\Upsilon(2S)$	—	—	—	—	1	0.068	0.07	0.038	0.319771
$\chi_{b2}(1P)$	—	—	—	—	—	1	—	—	0.22
$\chi_{b1}(1P)$	—	—	—	—	—	—	1	—	0.35
$\chi_{b0}(1P)$	—	—	—	—	—	—	—	1	0.06
$\Upsilon(1S)$	—	—	—	—	—	—	—	—	1

Table: NMEs for $\Upsilon(1S, 2S, 3S)$, and χ_{bJ}

n / n	PM	Fit JB	Fit JS	Fit KMR
$\langle \mathcal{O}^{\Upsilon(1S)}[^1S_0^{(8)}]\rangle$,GeV^3	$1.4 \cdot 10^{-1}$	0.0	0.0	0.0
$\langle \mathcal{O}^{\Upsilon(1S)}[^3S_1^{(1)}]\rangle$,GeV^3	$1.1 \cdot 10^{1}$	$1.1 \cdot 10^{1}$	$1.1 \cdot 10^{1}$	$1.1 \cdot 10^{1}$
$\langle \mathcal{O}^{\Upsilon(1S)}[^3S_1^{(8)}]\rangle$,GeV^3	$2.0 \cdot 10^{-2}$	$5.3 \cdot 10^{-3}$	0.0	0.0
$\langle \mathcal{O}^{\Upsilon(1S)}[^3P_0^{(8)}]\rangle$,GeV^5	0.0	0.0	0.0	$9.5 \cdot 10^{-2}$
$\langle \mathcal{O}^{\chi_{b0}(1P)}[^3S_1^{(8)}]\rangle$,GeV^3	$1.5 \cdot 10^{-2}$	0.0	0.0	0.0
$\langle \mathcal{O}^{\chi_{b0}(1P)}[^3P_0^{(1)}]\rangle$,GeV^5	2.4	2.4	2.4	2.4
$\langle \mathcal{O}^{\Upsilon(2S)}[^1S_0^{(8)}]\rangle$,GeV^3	0.0	0.0	0.0	0.0
$\langle \mathcal{O}^{\Upsilon(2S)}[^3S_1^{(1)}]\rangle$,GeV^3	4.5	4.5	4.5	4.5
$\langle \mathcal{O}^{\Upsilon(2S)}[^3S_1^{(8)}]\rangle$,GeV^3	$1.6 \cdot 10^{-1}$	0.0	0.0	$3.3 \cdot 10^{-2}$
$\langle \mathcal{O}^{\Upsilon(2S)}[^3P_0^{(8)}]\rangle$,GeV^5	0.0	0.0	0.0	0.0
$\langle \mathcal{O}^{\chi_{b0}(2P)}[^3S_1^{(8)}]\rangle$,GeV^3	$8.0 \cdot 10^{-3}$	$1.1 \cdot 10^{-2}$	0.0	0.0
$\langle \mathcal{O}^{\chi_{b0}(2P)}[^3P_0^{(1)}]\rangle$,GeV^5	2.6	2.6	2.6	2.6
$\langle \mathcal{O}^{\Upsilon(3S)}[^1S_0^{(8)}]\rangle$,GeV^3	$5.4 \cdot 10^{-2}$	0.0	0.0	0.0
$\langle \mathcal{O}^{\Upsilon(3S)}[^3S_1^{(1)}]\rangle$,GeV^3	4.3	4.3	4.3	4.3
$\langle \mathcal{O}^{\Upsilon(3S)}[^3S_1^{(8)}]\rangle$,GeV^3	$3.6 \cdot 10^{-2}$	$1.4 \cdot 10^{-2}$	$5.9 \cdot 10^{-3}$	$1.1 \cdot 10^{-2}$
$\langle \mathcal{O}^{\Upsilon(3S)}[^3P_0^{(8)}]\rangle$,GeV^5	0.0	$2.4 \cdot 10^{-2}$	$3.4 \cdot 10^{-3}$	$5.2 \cdot 10^{-2}$
χ^2/d.o.f	—	2.9	$2.7 \cdot 10^{1}$	$4.9 \cdot 10^{-1}$

$$\frac{\text{Color Octet Contribution}}{\text{Color Singlet Contribution}} \ll 1$$

$$v^2_{c\bar{c}} \simeq 0.3, \quad v^2_{b\bar{b}} \simeq 0.1$$

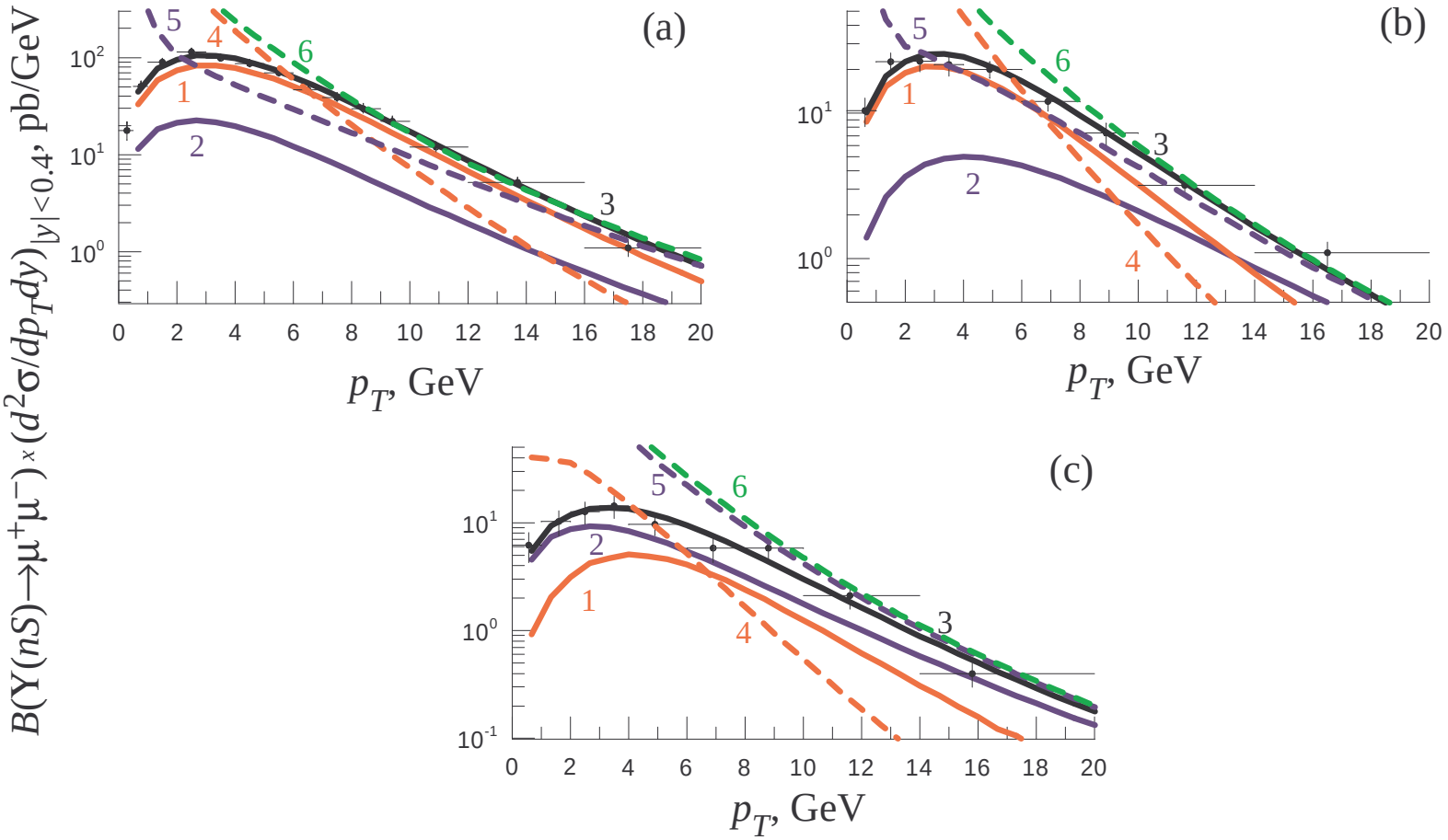

Prompt $\Upsilon(nS)$ p_T-spectra. $\Upsilon(1S)$– a, $\Upsilon(2S)$– b, $\Upsilon(3S)$– c, KMR distribution function

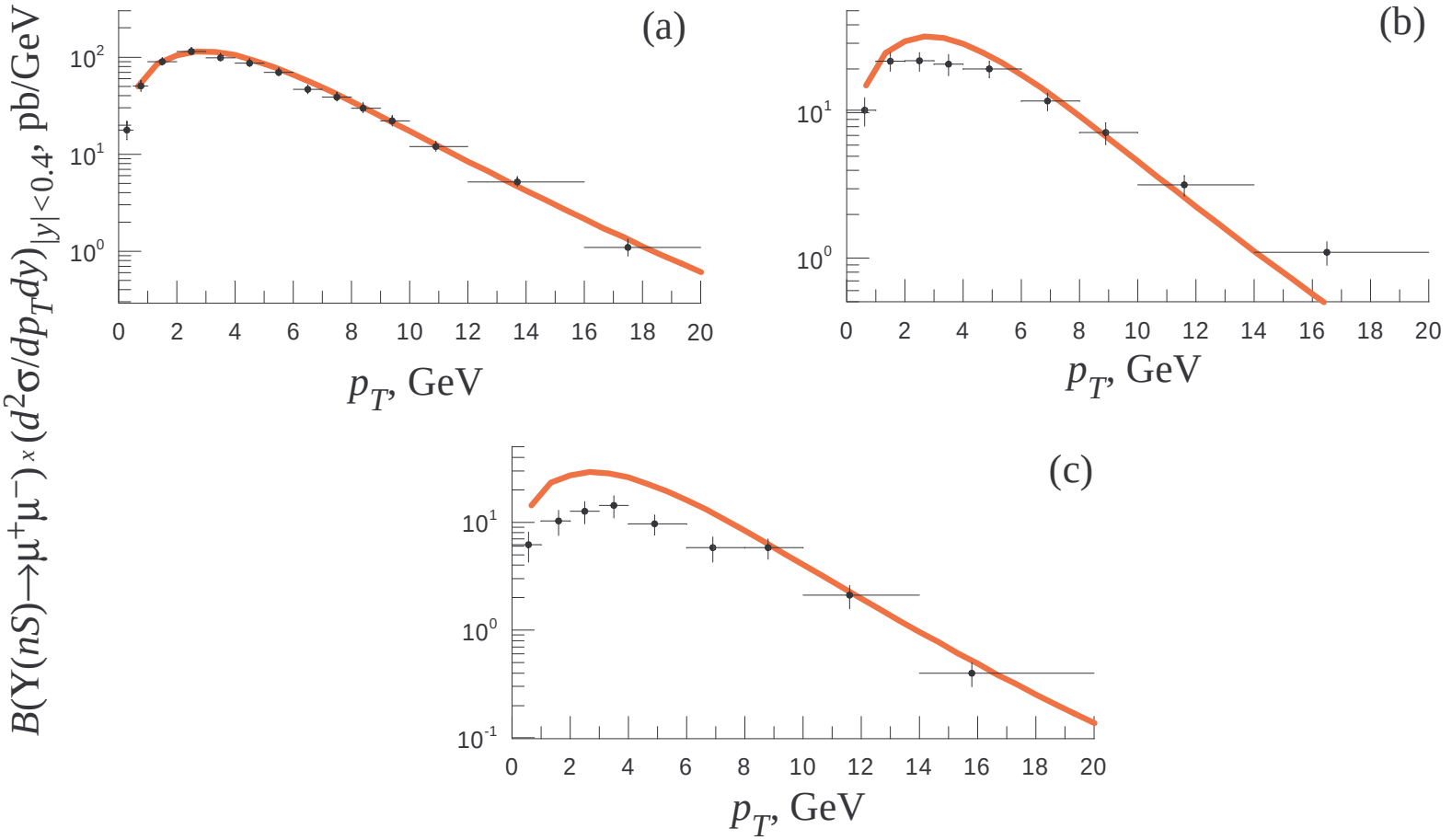

Prompt $\Upsilon(nS)$ p_T-spectra. $\Upsilon(1S)$– a, $\Upsilon(2S)$– b, $\Upsilon(3S)$– c, KMR distribution function, Color Singlet Model with $\chi_{bJ}(3P)$ contribution.

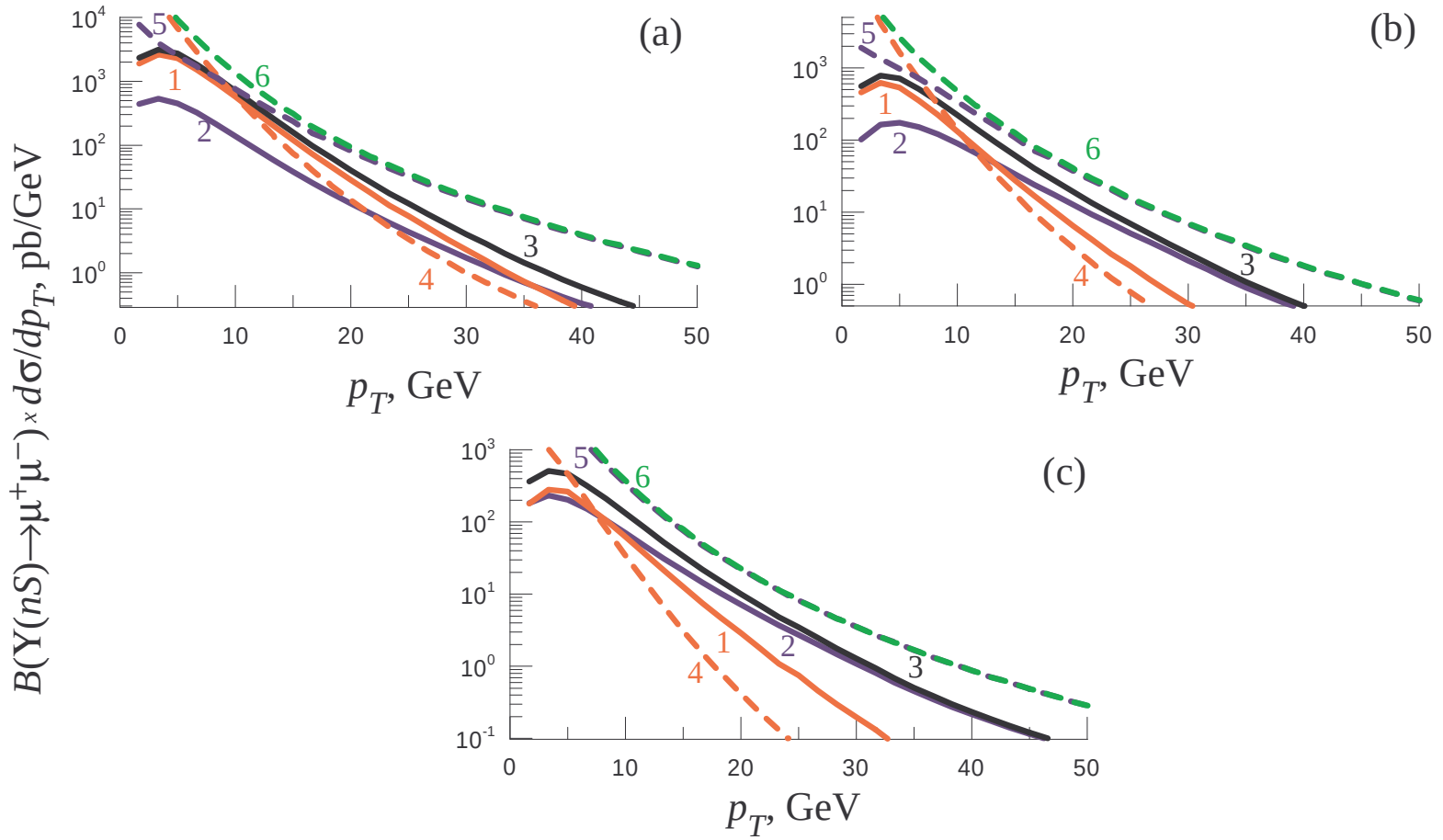

Prompt $\Upsilon(nS)$ p_T-spectra at the LHC. $\Upsilon(1S)$– a, $\Upsilon(2S)$– b, $\Upsilon(3S)$– c, KMR distribution function.

Conclusion

1. Working at LO in the QMRK plus NRQCD approach, we analytically evaluated the squared amplitudes of heavy quarks and direct heavy quarkonium production in two reggeized gluon collisions.

2. We extracted the relevant color-octet NMEs, $\langle \mathcal{O}^{\mathcal{H}}[^3S_1^{(8)}]\rangle$, $\langle \mathcal{O}^{\mathcal{H}}[^1S_0^{(8)}]\rangle$, and $\langle \mathcal{O}^{\mathcal{H}}[^3P_0^{(8)}]\rangle$ for $\mathcal{H} = \Upsilon(1S, 2S, 3S)$, J/ψ, ψ', $\chi_{cJ}(1P)$ and $\chi_{bJ}(1P, 2P)$, through fits to p_T distributions measured by the CDF Collaboration in $p\bar{p}$ collisions at the Tevatron with $\sqrt{S} = 1.8$ TeV and 1.96 TeV. Our fit to the Tevatron CDF data turned out to be satisfactory with the KMR unintegrated gluon distribution function in the proton.

3. $\triangle S \simeq \triangle L \simeq 0$.

4. $\langle \mathcal{O}^{(b\bar{b})}[^{2S+1}L_J^{(8)}]\rangle \ll \langle \mathcal{O}^{(c\bar{c})}[^{2S+1}L_J^{(8)}]\rangle$

5. We have described CDF data for $D-$meson p_T-spectra without free parameters using universal fragmentation functions by KKSS.

6. We have demonstrated the importance of gluon fragmentation in the $D-$meson production at the Tevatron and LHC Colliders.

6. We have predicted heavy meson and heavy quarkonium production p_T-spectra at the LHC Collider in the framework of QMRK approach.

7. We have demonstrated phenomenological application of the QMRK approach for heavy quark and heavy quarkonium production at high energies.